Anaerobic membrane bioreactors (AnMBR) treating urban wastewater in mild climates

Ángel Robles [a], Freddy Durán [b], Juan Bautista Giménez [c], Emérita Jiménez [b], Josep Ribes [a], Joaquín Serralta [c], Aurora Seco [a], José Ferrer [c], Frank Rogalla [b]

[a] CALAGUA – Unidad Mixta UV-UPV, Departament d'Enginyeria Química, Universitat de València, Avinguda de la Universitat s/n, 46100 Burjassot, Valencia, Spain.

[b] FCC Aqualia, S.A., Avenida Camino de Santiago, 40, 28050 Madrid, Spain.

[c] CALAGUA – Unidad Mixta UV-UPV, Institut Universitari d'Investigació d'Enginyeria de l'Aigua i Medi Ambient – IIAMA, Universitat Politècnica de Valencia, Camí de Vera s/n, 46022 Valencia, Spain.

Abstract

Feasibility of an AnMBR demonstration plant treating urban wastewater (UWW) at temperatures around 25-30 ºC was assessed during a 350-day experimental period. The plant was fed with the effluent from the pre-treatment of a full-scale municipal WWTP, characterized by high COD and sulfate concentrations. Biodegradability of the UWW reached values up to 87%, although a portion of the biodegradable COD was consumed by sulfate reducing organisms. Effluent COD remained below effluent discharge limits, achieving COD removals above 90%. System operation resulted in a reduction of sludge production of 36-58% compared to theoretical aerobic sludge productions. The membranes were operated at gross transmembrane fluxes above 20 LMH maintaining

low membrane fouling propensities for more than 250 days without chemical cleaning requirements. Thus, the system resulted in net positive energy productions and GHG emissions around zero. The results obtained confirm the feasibility of UWW treatment in AnMBR under mild and warm climates.

Keywords

Anaerobic membrane bioreactor (AnMBR); industrial-scale membrane; demonstration plant; methane production; urban wastewater (UWW); mild/warmer climate

1. Introduction

Global energy crisis and climate change drives WWTPs towards the implementation of more cost-effective and cleaner technologies, to replace current energy-intensive aerobic processes that require considerable energy input for organics oxidation (Lee et al., 2017). Hence, it is highly necessary and urgent to apply new water management models focused on Circular Economy (CE), to palliate water scarcity issues and reduce carbon footprint and depletion of resources such as fossil fuels or minerals. CE transforms current linear economic models based on extraction, use and final disposal of non-renewable raw-materials into a self-sufficient cradle-to-cradle bio-based economy. Hence, urban, agricultural, and industrial residue must be regarded as valuable raw materials rather than as a waste.

Nutrient recycling from waste to farmland is one of the pillars of CE, particularly phosphorus, because it is an essential and irreplaceable element in the production of crops (Robles et al., 2019). The energy-intensive Haber-Bosch process used to produce urea fertilizer mostly depends on fossil fuels, significantly affecting environmental

sustainability. On the other hand, phosphorus deposits are unequally distributed worldwide, with the top four countries extracting around 80 %, and only 12 countries having significant production. This could cause geopolitical conflicts when scarcity rises, and even today fertilizer quality issues are frequent (Günther et al., 2018). Hence, a CE context favors non-nutrient-destructive technologies such as anaerobic processes, allowing nutrient recovery and/or nutrient recycle and reuse by e.g. microalgae cultivation, fertigation, membrane contactors, etc. (Robles et al., 2019).

The switch from aerobic to anaerobic processes broadens the recovery potential of wastewater, and avoids the higher net energy demands of aerobic treatment (Ince et al., 2017). Anaerobic solutions can be energy-neutral or even be net energy producers despite treating low-loaded UWW (Perry L McCarty et al., 2011). Reducing net energy demand implies a reduction in both use of mineral carbon and greenhouse gases (GHG) emissions.

Anaerobic digestion (AD) eliminates energy input related to aeration for the removal of organics, transforms biodegradable organic matter into the gaseous energy carrier CH_4, produces less biosolids to be handled, and has the potential for nutrient recovery (Batstone and Virdis, 2014; van Lier et al., 2019). However, AD can present some issues depending on the operating conditions (e.g. treatment flow rate, temperature, etc.) and the waste to be treated (e.g. low-strength wastewaters, etc.) mainly due to the low growth rate of anaerobic microorganisms at sub-mesophilic temperatures and their sensitivity to process dynamics (Robles et al., 2018). On the one hand, hydrolysis and microorganism growth-rates are rapidly reduced as temperature drops, making it necessary to increase the sludge retention time (SRT) to counterbalance the low

microbial activity at low temperatures. However, UWW flows are generally high and a SRT increase would result in very large AD working volumes when biomass is not immobilized. On the other hand, Martin et al. (2011) reported that influent COD concentrations in the range of 4 to 5 g $COD \cdot L^{-1}$ are necessary to anaerobically produce the biogas that would provide enough energy upon combustion to warm an anaerobic reactor at 15ºC up to mesophilic conditions (i.e., 35 ºC). Nevertheless, UWWs are generally low- to middle-loaded and an exogenous energy source would be needed to treat it anaerobically. Consequently, the typically high production rates of UWW would require of large amounts of energy to warm the reactor up to mesophilic conditions. Therefore, anaerobic treatment of UWW at ambient temperature is essential to enhance sustainability. Indeed, anaerobic treatment of UWW has only been carried out efficiently in mild climates, where the high temperature enables anaerobic treatment of UWW at ambient temperature to be feasible without the application of an exogenous energy source (Lew et al., 2011). In this respect, combining AD with membrane technology in the so-called AnMBR is a promising solution for treating different types of waste (Becker et al., 2017; Dereli et al., 2012; Galib et al., 2016; Kamali and Khodaparast, 2015; Ozgun et al., 2013). This combination has intrinsic advantages: the use of membranes for decoupling the solids retention time (SRT) and the hydraulic retention time (HRT), and the inherent retention of solids, generating a high quality effluent (Krzeminski et al., 2017). Increased biomass retention compensates for reduced growth rates of anaerobic microbes, favoring their application to a wider range of temperatures (Stazi and Tomei, 2018).

Hence, AnMBR presents a number of advantages that could help turning UWW into a

source of energy, nutrients, and recyclable water (Robles et al., 2018): i) retains anaerobic microbes completely since the HRT and the SRT are uncoupled, preventing washout of the slow-growing methane-forming methanogens while reducing footprint; ii) allows ambient-temperature AD operation by increasing SRT and leads to a lower amount of biosolids to dispose; iii) produces excellent quality permeate because of micron level filtration of the effluent regardless of its initial quality; iv) is non-nutrient-destructive allowing for its recovery or direct reuse in effluent; v) transforms biodegradable organics into the gaseous energy carrier CH_4 to be used as energy source, with no external energy demands, which reduces GHG emissions by saving energy consumption .

However, to boost the widespread application of AnMBR as core technology for UWW treatment some issues need to be further addressed, such as: i) the concentration of methane dissolved in the effluent, which needs to be captured both to prevent its stripping to the atmosphere downstream and to enhance energy recovery (Giménez et al., 2012; Smith et al., 2012); ii) membrane fouling, which reduces system productivity and increases cleaning requirements, thus reducing membrane lifespan at higher operating expenses (Robles et al., 2013); and iii) the competition between sulfate reducing bacteria (SRB) and methanogens for the available substrate (Giménez et al., 2011). This competition could affect the feasibility of AnMBR for UWW because of different factors, such as the reduction of the quantity and quality of the produced biogas thus reducing energy harvesting from wastewater, and the toxicity to anaerobic microorganisms because of the presence of H_2S in the liquid.

Although AnMBR technology is currently used to treat industrial effluents (Dereli et al.,

2012), full scale applications for UWW have not yet been reported (Shin and Bae, 2018). Various authors have evaluated the performance of different AnMBR pilots (*e.g.* Aslam et al., 2017; Giménez et al., 2011; Gouveia et al., 2015; Kim et al., 2011; Li and Wang, 2006; Martin Garcia et al., 2013; Martinez-Sosa et al., 2011; Shin et al., 2014; Wang et al., 2018). However, it is essential to increase Technology Readiness Level (TRL) to demonstrate the feasibility of AnMBR technology for full-scale UWW treatment. In this sense, obtaining realistic experimental data operating as close to full-scale conditions as possible is paramount to accurately validate scalability issues in terms of technical, economic and environmental feasibility of AnMBR technology.

In this work, an industrial prototype (demonstration scale, TRL of 6) was operated to assess the technical, economic and environmental feasibility of AnMBR for UWW treatment. This plant was fed with effluent from the pre-treatment of the "Alcázar de San Juan" WWTP (Alcázar de San Juan, Ciudad Real, Spain). This wastewater was characterized by a high organic load and a high sulfate concentration, which favors the competition of sulfate reducing bacteria (SRB) and methanogens for the available substrate. The design characteristics and scale of this demonstration plant is considered adequate to give good performance data for scaling-up AnMBR to full-scale UWW treatment, since it incorporates commercial full-scale hollow-fiber membrane modules and all the elements required to address the abovementioned key issues. Hence, this research aims at demonstrating the potential of AnMBR as alternative to conventional treatment of UWW in mild climate regions. To this aim, key process indicators are evaluated (i.e. organics removal, sludge production, energy recovery, energy demand, and GHG emission), which validation is needed to accurately demonstrate the technical,

economic and environmental feasibility of AnMBR technology for UWW treatment at full-scale.

2. Materials and methods

2.1. AnMBR description

Figure 1a shows the flow diagram of the AnMBR operated in this work. This demonstration plant (Figure 1) mainly consists of an anaerobic reactor (AnR) of 40 m^3 (34.4 m^3 working volume + 5.6 m^3 headspace) connected to three membrane tanks (MT) of 0.8 m^3 each (0.7 m^3 working volume + 0.1 m^3 headspace). Each membrane tank is fitted with one ultrafiltration membrane module (PURON® PSH41, KMS, 0.03-µm pore size, total filtration area of 41 m^2), giving a total filtration area of 123 m^2. A sieve screw (RF, 1.5-mm screen size), an equalization tank (ET, 1.1 m^3) and a clean-in-place (CIP) tank (0.37 m^3) are also included as main elements of the plant. Figure 1b shows an overview of the system, which was located in the "Alcázar de San Juan" full-scale WWTP (Alcázar de San Juan, Ciudad Real, Spain). A 2.1-m^2 degassing membrane (DM) unit for dissolved methane recovery from the AnMBR permeate was used in this study, consisting in a hollow-fiber commercial module of polydimethylsiloxane (PDMS) provided by PermSelect®, MedArray Inc. USA.

2.2. AnMBR monitoring and control

Different on-line sensors and measurement equipment were installed in the plant to obtain real-time information of the state of the process. The on-line sensors installed in the AnMBR were: (i) eight liquid-flow-rate transmitters (electromagnetic type), one for each pump; (ii) four gas-flow-rate transmitters (vortex type), located in the gas inlets to

anaerobic reactor and membrane tanks; (iii) five level transmitters (hydrostatic type), installed in membrane tanks, anaerobic reactor, equalization tank and CIP tank; (iv) three liquid pressure transmitters (gauge pressure type), installed in the permeate lines of each MT in order to monitor the transmembrane pressure (TMP); two gas pressure transmitters (gauge pressure type), which monitored the header pressure of the biogas distributions system; one pH-T and one ORP sensor, located in the internal sludge recycling of the anaerobic reactor; two solids concentration transmitters (modified absorption type), located in anaerobic reactor and equalization tank; one biogas analyzer to monitor biogas composition (CH_4, CO_2, O_2 and H_2S); and one gas meter (pulse measurement) to monitor biogas production. Concerning actuators, the plant was equipped with ten variable speed drives to control the rotating speed of the pumps (P-1, P-2, P-A1, P-B1, P-C1, P-A2, P-B2 and P-C2) and the blowers (C-1 and C-2), as well as a set of automatic valves to control plant performance.

Besides the on-line process monitoring, the following parameters were determined: total and soluble COD (COD_T and COD_S, respectively), volatile fatty acids (VFA), alkalinity (Alk), sulfate (SO_4-S), sulfide (HS^-), total nitrogen (N_T), total phosphorus (P_T), nitrate (NO_3^-), phosphate (PO_4^{-3}), total suspended solids (TSS), and volatile suspended solids (VSS). 24-hour-composite samples were taken twice a week from the influent for all measurements except COD_T, N_T, P_T and TSS, which were analyzed daily. Grab samples were taken twice a week from the effluent and mixed liquor.

2.3. AnMBR operation

The demonstration plant was fed with effluent from the pre-treatment of the “Alcázar de

San Juan" full-scale WWTP (Alcázar de San Juan, Ciudad Real, Spain). The pre-treatment step of the full-scale facility consisted of screening and sand removal. Following an additional pre-treatment of the wastewater in a sieve screw and homogenization in the equalization tank, the wastewater was pumped into the anaerobic reactor. The main characteristics of the influent were 1235 ± 462 mg $COD \cdot L^{-1}$, 536 ± 248 mg $TSS \cdot L^{-1}$ and 164.4 ± 31.3 mg $SO_4\text{-}S \cdot L^{-1}$. BOD measured at 5 days was 694 ± 281 mg $BOD \cdot L^{-1}$. It is important to highlight the relatively high COD and sulfate concentrations that were due to the contributions of several nearby dairy and wine industries, as well as the strong variability of the influent load, which enabled to validate the applicability of AnMBR technology under a wide range of influent conditions.

The mixed liquor from the anaerobic reactor was continuously recycled through the membrane tanks, where the effluent was obtained by vacuum filtration. A fraction of the biogas produced in the system was recycled to the reactor through coarse bubble diffusers for stirring purposes. This stirring strategy favored the stripping of dissolved gases from the liquid phase, thus avoiding oversaturation of methane in the effluent (Giménez et al., 2012). Another fraction of the produced biogas was recycled to the membrane tanks for membrane scouring purposes giving additional gas stripping effect. In order to recover the biogas bubbles extracted with the membrane effluent, a degassing vessel (DV in Figure 1a) was installed between each membrane tank and the CIP tank. Moreover, degassing membranes (DM in Figure 1a) were used to recover the remaining methane dissolved in the effluent.

The membrane tanks were operated according to a specific schedule involving a

combination of different individual stages taken from a basic filtration-relaxation (F-R) cycle. Besides filtration and relaxation, membrane operation included back-washing, degasification and ventilation stages (Robles et al., 2015). The membrane operation automation enabled to optimize the frequencies and lengths of the different membrane operating stages.

Table 1 summarizes the operating conditions set during the experimental period of the AnMBR plant. The system was started up on September 2016. This work shows the operation of the system during 350 days in continuous mode in order to evaluate the potential of AnMBR technology for high-loaded UWW treatment in mild and warmer climates. To this aim, the reactor was inoculated with 20 m^3 (60% of reactor volume) of sludge from the anaerobic digester of a municipal WWTP located in Toledo. The system was filled up to 36.5 m^3 of total working volume (reactor plus membrane tanks) with UWW coming from the pre-treatment of the "Alcázar de San Juan" full-scale WWTP. The HRT was set firstly to around 60 hours without sludge wasting during the first 65 days in order to allow the biomass to acclimatize to the system conditions. During this period, the temperature in the reactor was set to 30 ºC. Then, a minimum temperature set point of 27 ºC was established during the end of fall, the whole winter and the beginning of spring seasons. The temperature control was turned off for the rest of the year. Thus, the temperature was maintained around 27 ºC during the whole experiment in order to simulate mild climate conditions. Once the biomass in the reactor was developed, the SRT was sequentially reduced from 190 to 120 and to 70 days, while the HRT was modified from 60 to 24 and 40 hours.

Regarding membrane operation, the gross 20ºC-standardised transmembrane flux (J_{20})

was modified between 15 and 25 LMH. The biogas sparging intensity for membrane scouring measured as specific gas demand per permeate volume (SGD_P), was ranged from 15 to 20 $Nm^3_{BIOGAS} \cdot m^{-3}_{PERMEATE}$.

2.4. Analytical methods

TSS, VSS, chemical oxygen demand (COD), biological oxygen demand (BOD), sulfate, sulfide, and nutrients were determined according to Standard Methods (APHA, 2005). VFA concentration was determined by titration according to the method proposed by Moosbrugger et al. (1992).

The concentration of methane dissolved in the effluent from the AnMBR was determined through the head-space method described by Giménez et al. (2012). The methane fraction reached in head-space vials was determined through a gas chromatograph, which was equipped with a flame ionization detector (GC-FID, Thermo Scientific). The column used was a 30 m x 0.319 mm x 25 μm HP-MOLESIEVE column (Agilent Technologies), which was operated at 40 ºC, using helium as carrier gas at a flow rate of 40 $mL \cdot min^{-1}$. It was injected 0.1 mL of gas samples in the gas chromatograph, using methane pure gas (99.9995%) as standard gas.

2.5. Data processing and calculations

To evaluate the performance of the biological process, the methane yield was calculated as the amount of methane produced per unit of influent COD, both not accounting for the methane that could theoretically be recovered from permeate by means of (Eq. 1) and accounting dissolved methane by means of (Eq. 2), respectively:

$$Y_{CH_4}^{BG} = \frac{V_{CH_4}^{BG}}{COD_{in}}$$ Eq. 1

$$Y_{CH_4}^{BG+PERM} = \frac{V_{CH_4}^{BG+PERM}}{COD_{in}}$$ Eq. 2

Where, $V_{CH_4}^{BG}$ is the daily volumetric production measured in standard conditions (STP) of methane recovered in the biogas (m^3 STP·d^{-1}), $V_{CH_4}^{BG+PERM}$ is the daily volumetric production measured in standard conditions (STP) of methane both recovered in the biogas and dissolved in the permeate (m^3 STP·d^{-1}) and COD_{in} is the concentration of COD in the influent (kg COD·d^{-1}).

The concentration of methane dissolved in the effluent was calculated using the experimentally-determined head-space gas fraction by means of the following equation (Giménez et al., 2012):

$$[CH_4]_{dis} = \left(\frac{V_G}{V_L \cdot R \cdot T} + \frac{M^W}{H^{CH4}(T) - P \cdot y^{CH4}}\right) \cdot P \cdot \bar{M}^{CH4} \cdot y^{CH4}$$ Eq. 3

Where $[CH_4]_{dis}$ is the concentration of methane dissolved in the effluent, V_G and V_L are the gas and liquid volumes in collected vials (L), R is the universal constant of gases (0.082 atm·L·mol^{-1}·K^{-1}), T is the temperature of stored vials (K), M^W is the pure water molarity (55.56 mol·L^{-1}), P is the total pressure of stored vials (atm), M^{CH4} is the methane molecular weight (16 g·mol^{-1}), $H^{CH4}(T)$ is the Henry's constant for methane, and y^{CH4} is the experimentally-determined head-space gas fraction. This Henry's constant depends on temperature and can be calculated according to the following equation:

$$H^{CH4}(T) = 10^{\left(\frac{-675{,}74}{T(K)}+6{,}88\right)} \quad \text{Eq. 4}$$

Regarding the filtration process, the measured gross transmembrane flux was standardized to 20 ℃ according to Eq. 5:

$$J_{20} = J \cdot e^{-0.0239\cdot(T-20)} \quad \text{Eq. 5}$$

Where, J_{20} is the 20 ºC-standardized gross flux, J is the gross flux and T is the temperature in Celsius.

The fouling rate due to cake-layer formation (FR_C) was calculated during filtration stages using a classical regression model according to Eq. 6:

$$FR_C = \frac{\partial TMP_C}{\partial t} = \frac{n\cdot\sum_1^n\left(TMP_{C,i}\cdot t_i\right)+\sum_1^n TMP_{C,i}\cdot\sum_1^n t_i}{n\cdot\sum_1^n {TMP_{C,i}}^2-\left(\sum_1^n TMP_{C,i}\right)^2} \quad \text{Eq. 6}$$

Where, TMP_C is the TMP measured during filtration stages, and t is the sampling time, which are evaluated for n times (one sampling each 5 seconds) during each filtration stage

Energy balances for this AnMBR system were performed as shown in Jiménez-Benítez et al. (2020). Energy recovery from biogas was calculated assuming a CHP-technology electric efficiency of 35%. Heating-energy input was not considered in the energy balance since the system was operated to simulate mild-climate conditions. The potential energy output from dissolved methane capture was also considered for net energy demand calculations. Specifically, two different cases were evaluated: (a) dissolved methane not being captured, and (b) dissolved methane being captured with a

recovery efficiency of 69% using degassing membranes. This dissolved methane recovery efficiency was experimentally determined in the system when establishing a pay-back period of 10 years for the degassing membrane system as design target (Sanchis-Perucho et al., 2020).

Greenhouse gases (GHG) emissions were assessed by calculating equivalent CO_2 emissions during the operation phase. Direct GHG emissions were related to dissolved methane emissions, while indirect GHG emissions were related to power requirements. A 100-year horizon global warming potential (GWP) of 34 kg CO_2 equivalent per kg of emitted methane was considered in this study. This value was extracted from the globally accepted Life Cycle Impact assessment model ReCiPe 2016 (Huijbregts et al., 2016). According to IPCC Guidelines for National Greenhouse Gas Inventories (Eggleston H.S., Buendia L., Miwa K., 2006), biogenic CO_2 emissions from wastewater were not taken into account for GHG calculation. In this respect, CO_2 from the combustion or decay of short-lived biogenic material removed from where it was grown is reported as zero in the Energy and Waste Sectors (for example CO_2 emissions from biofuels, and CO_2 emissions from wastewater). This is due to the reduced life-cycle of biogenic CO_2. Indirect CO_2 emissions from power energy generation were calculated considering a specific Spanish electricity emission factor of 0.392 kgCO_2 per kWh.

3. Results and discussion

3.1. Start-up period of the plant

The system was operated in batch mode for 25 days, period during which the wastewater was introduced to the system progressively until reaching the total working

volume. Once the reactor reached the operating volume and stable TSS concentrations were achieved, the HRT was set to 60 hours. The operating temperature was controlled to 30 ºC and no sludge was wasted in order to retain as much active biomass as possible during the acclimatization to the new environment. The methane content in the biogas increased progressively during the first weeks of operation and, by day 30, a plateau was reached around 65-70% of methane content. Moreover, the analytical control showed that the VFA content in the effluent remained negligible, indicating that anaerobic microbes adapted adequately to the operating and environmental conditions. Additionally, the on-line monitoring revealed stable mixed liquor pH values between 6.8 to 7.2 without applying any control action, while the ORP remained stable between -500 and -400 mV.

3.2. Biological process performance

Once the system was fully operational around day 65, the HRT was reduced from 60 to 24 hours. As can be seen in Figure 2a, the sudden change in the HRT combined with a slight decrease in temperature (*i.e.* the temperature control was turned off) resulted in an organic overloading that unbalanced the different stages of the anaerobic degradation, as it was evidenced by the accumulation of VFA (see Figure 2a). Around day 80, the HRT was increased from 24 to 40 hours to favor VFA consumption, and the SRT was set to 190 days. On day 95, the SRT was reduced to 120 days, and the system was allowed to evolve under these new operational conditions. The steady operation of the system contributed to reestablish a balanced performance that led to the consumption of the previously accumulated VFA. Around day 100, both the effluent COD and TSS concentration values were quasi-stable, indicating the vicinity of a pseudo-steady state.

Completely steady performance was not expected as a result of the strong variability observed in the influent composition (see Figure 2b). Around day 170, the SRT was further reduced to 70 days. However, the operational disturbance was not significant to the system performance, which remained unchanged at the pseudo-steady state achieved previously. The TSS concentration slightly fluctuated around 10 $g \cdot L^{-1}$ whereas the VFA concentration remained virtually negligible for the whole experimental period. In addition, as Figure 2b shows, effluent COD concentration mostly remained below effluent discharge limits in spite of the strong dynamics of the influent COD, resulting in an average COD removal efficiency around 92%. The obtained results show the feasibility and highlight the robustness of the AnMBR system for UWW treatment in mild and warmer climates. Indeed, a number of studies involving a wide range of substrates have underlined the ability of AnMBR for removing organics (Smith et al., 2012; Song et al., 2018). However, unlike most of the pilot scale studies, the solids concentration in the demonstration scale system was not affected by the increase in the SRT that remained stable around 8 $g \cdot L^{-1}$.

Figure 3 shows the evolution of sludge production, methane yield, total COD biodegraded and the fraction of the biodegraded COD consumed by SRB. This figure shows pronounced fluctuation in the parameters, which were calculated on a weekly basis. This strong fluctuation reflects the high variability of the influent COD, as also evidenced by the OLR entering the system.

Methane yield was also determined both as the amount of methane recovered with the biogas, and as the total amount of methane produced (recovered with the biogas and dissolved in the effluent), yielding values of 193.0 ± 51.2 and 210.2 ± 51.3 L_{CH4}

$STP \cdot kg^{-1}$ COD_{in}, respectively. As Figure 3a shows, the amount of methane lost in the effluent was low since the system was operated at high ambient temperatures, resulting in reduced methane solubility and high methane recoveries with the biogas. Taking into account that 350 L STP of CH_4 are theoretically produced per kg of COD degraded by methanogens, the methane yield obtained revealed a biomethane potential of the influent wastewater around 60 %. However, as illustrated in Figure 3b, a portion of the biodegradable COD was consumed by SRB to carry out dissimilative sulfate reduction (DSR) to sulfide. At the end of the experimental period, the average COD consumption by SRB accounted for approx. 37 % of COD biodegraded (see Figure 3b).

Sulfate-rich wastewaters are typical of Mediterranean coastal areas already. Indeed, according to Lens et al. (1998), the sulfate content in UWW typically range from 2 to 170 mg SO_4^{2-}-$S \cdot L^{-1}$. Thus, the influent sulfate concentration to the AnMBR averaged at the end of this typical range. This was likely due to a significant dairy- and wine-industries contribution, which use sulfur compounds in several operations of the production cycle, resulting in an even higher sulfate concentration. Indeed, COD removal by SRB reached values above 50% during the experimental period due to the high influent sulfate concentration. DSR-consumed COD is also biodegradable and would have ended-up as methane provided no sulfate would have been present. Therefore, the overall biodegradability of influent wastewater (considering both the COD consumed by methanogens and SRB) reached values up to 85 % in average.

Although a significant competition between SRB and methanogens was observed, SRB and methanogenic activities were not significantly inhibited during the experimental period as highlighted by the high COD removal efficiencies achieved. Moreover, VFA

accumulation was not detected. On the other hand, the produced sulfide was distributed between H_2S and the ionic species HS^- and S^{2-}. According to Maree and Strydom (1985), the undissociated form is responsible of activity inhibition, since only uncharged molecules can permeate the cell wall. In this study, the pH in the mixed liquor varied from 7.2 to 6.8, resulting in H_2S concentrations between 42% and 65% of total sulfide, respectively, calculated from a pKa of 6.9 for the first dissociation equilibrium of H_2S. Therefore, maximum H_2S concentrations of around 105 mg H_2S-$S \cdot L^{-1}$ were reached. When comparing this value with the 50% H_2S inhibitory concentrations reported in literature, it can be concluded that SRB and methanogenic activities were not significantly affected by H_2S during the experimental period. For instance, Fedorovich et al. (2003) reported 50% H_2S inhibitory concentrations of 213 and 245 mg H_2S-$S \cdot L^{-1}$ for hydrogenotrophic and acetotrophic methanogens, while sulfate reducers activity was half inhibited at H_2S concentrations of 265 mg H_2S-$S \cdot L^{-1}$. Regarding the sludge production, following a start-up period without any sludge wasting (around day 80), the SRT was decreased stepwise down to 190, 120 and, eventually, to 70 days. From day 280, COD accumulation was negligible, resulting in an average waste-sludge production of 0.144 ± 0.021 kg VSS per m^3 of treated water (0.136 ± 0.054 kg $VSS \cdot kg^{-1}$ COD_{in}) when operating at SRT of 70 days and HRT of 40 hours. Unstabilized sludge production in aerobic activated-sludge systems treating UWW accounts for around 0.23-0.35 kg VSS per kg COD removed (Foladori et al., 2010). Therefore, considering an average COD removal efficiency around 92%, the reduction in sludge production from the system stands for approx. 36-58% of that produced aerobically. On the other hand, waste sludge production in aerobic WWTPs including sludge stabilization accounts for around 0.18 kg VSS per kg COD removed

(Foladori et al., 2010), revealing that a minimum reduction in sludge production of 18% is possible compared to aerobic technologies. Moreover, the sludge production in the present study is 30% lower than that obtained by Seco et al. (2018a), also working with an AnMBR pilot plant treating low-loaded UWW at similar temperature conditions (27ºC) and 140 days of SRT. The difference was attributed to the higher influent wastewater biodegradability, which was 24 % higher than the value reported by Seco et al. (2018a), which resulted in 68.5%. In the absence of an electron sink, the metabolic energy gain of microorganisms is limited. Indeed, most of the energy contained in the substrates is derived to the products, during the so-called substrate level phosphorylation, and only a small amount is devoted to anabolism. Thus, biomass yields of anaerobic microorganisms are very low, and most of the metabolized substrates will end up as biogas. Therefore, in the case of UWW, which contains a considerable fraction of particulate COD, a higher biodegradability leads to a lower sludge production. The main benefits of AnMBR technology (biogas production, low sludge production) increase at high influent wastewater loads.

3.3. Filtration process performance

Figure 4 shows the evolution of the daily average values for TMP, J_{20}, SGD_P, the 20ºC-strandardized membrane permeability (K_{20}) and FR_C. During the experimental period, the membranes were operated at two different regimes (see Figure 4b). Sub-critical filtration conditions were established from around day 25 to 160 (see Figure 4c), maintaining transmembrane fluxes below the critical one; J_{20} was around 15-17 LMH

with SGD_P from approx. 12 to 17 $Nm^3_{BIOGAS} \cdot m^{-3}_{PERMEATE}$. From day 160 to 335, sub-critical/critical filtration conditions were established (see Figure 4c); J_{20} was set to 20.5-23.5 LMH and SGD_P was around 17.5 (days 160-205), 15.5 (days 205-220), and 13.0 (days 220-270) $Nm^3_{BIOGAS} \cdot m^{-3}_{PERMEATE}$. At the end of the experimental period (days 335-350), sub-critical filtration conditions were re-established (see Figure 4c); J_{20} was around 18 LMH with SGD_P around 16 $Nm^3_{BIOGAS} \cdot m^{-3}_{PERMEATE}$. After the start-up period, the TSS concentration entering the membrane system remained around 8 $g \cdot L^{-1}$.

As Figure 4b shows, a significant TMP increase was observed when a step increase of 5 LMH was applied to the transmembrane flux, *i.e.* J_{20} was increased from 17 (sub-critical) to 23 LMH (sub-critical/critical). As common resistance-in-series models predict, a higher resistance to flux was observed by increasing J_{20}. This effect can also be observed in K_{20}, since TMP and K_{20} are inversely proportional. Moreover, the irreversible fouling rate (referred here as the time slope of TMP during the experimental period) raised as a result of operation in the vicinity of critical-filtration conditions. In this respect, Figure 4b illustrates that TMP increased from 50 (the base value measured due to the intrinsic membrane resistance) to around 100 mbar from day 25 to 160, resulting in an irreversible fouling rate of around 0.37 $mbar \cdot day^{-1}$. On the other hand, a TMP increased from 215 to 475 mbar from day 160 to 270, resulting in an average irreversible fouling rate of around 2.2 $mbar \cdot day^{-1}$. Nevertheless, two different FR_C were observed within days 160 and 270. This change observed on fouling rate was the result of decreasing the SGD_P from 15.5 to 13 $Nm^3_{BIOGAS} \cdot m^{-3}_{PERMEATE}$ on day 223, highlighting the potential of gas sparging for membrane fouling mitigation. Indeed, as Figure 4c shows, the highest FR_C values for MT-A were recorded from day 230 to 275.

MT-A was stopped within days 270 and 335 for validating the obtained results by running MT-B. Hence, this tank was operated at similar J_{20}, SGD_P and TSS values than the ones set in MT-A within days 220 and 270. Similar fouling rates for both reversible (FR_C) and irreversible mechanisms were reached when working at similar operating conditions (see Figure 4b ad Figure 4c), thus validating the results obtained in MT-A.

Besides the decrease in K_{20} (*i.e.* TMP increase), irreversible fouling rate remained at low values even when the J_{20} was increased and the SGD_P was reduced. Hence, the results obtained show that it is possible to operate the membranes at gross transmembrane fluxes above 20 LMH maintaining low membrane fouling propensities. Moreover, after operating the membrane for more than 250 days no significant irreversible fouling problems were detected, thus no chemical cleaning was required. Indeed, MT-A was re-started on day 335 with J_{20} of 18 LMH and SGD_P of 16 $Nm^3_{BIOGAS} \cdot m^{-3}_{PERMEATE}$ without applying any chemical cleaning procedure, recording a slight increase in membrane permeability due to the removal of remaining reversible fouling through membrane scouring by gas sparging. Overall, competitiveness of the filtration process was achieved when comparing with other AnMBR systems (see e.g. van Lier et al., 2019).

In conclusion, it was possible to keep the filtration process running satisfactorily even at SGD_P of 14 $Nm^3_{BIOGAS} \cdot m^{-3}_{PERMEATE}$. Therefore, low power requirements related to filtration were achieved, *i.e.* around 0.15 kWh per m^3 of treated water. Moreover, it is worth to point out that pathogen levels detected in AnMBR effluents are close to those that would be acceptable for disinfection-free reuse of the reclaimed water based on quantitative microbial-risk assessment. Indeed, Harb and Hong (2017) reported Log

removal values of 6.9, 6.6, 6.8, and 7.0, for total coliform, faecal coliform, *E.coli*, and enterococci, respectively. On the other hand, Seco et al. (2018b) reported that nor *E.coli* cfu per 100 mL neither helminthic eggs are detected in the effluent from an AnMBR equipped with ultrafiltration membrane units with a mean pore size of 0.03 μm. Thus, reclaimed water could be produced in the system, which could be used for different purposes, i.e. agricultural irrigation, aquifer recharge, urban or industrial uses, recreational areas. Therefore, additional costs and energy input needed for disinfecting the effluent is avoided compared to other systems (*e.g.* conventional activated sludge).

3.4. Energy demand and GHG emissions

As commented before, power energy requirements for pumps and blowers were theoretically calculated. To this aim, different measures from the plant were used as inputs, *i.e.* gas flow rate, gas temperature, gas pressure, permeate flow rate, transmembrane pressure, tank heights, etc. Figure 5a shows the theoretically-calculated net energy demand of the AnMBR plant.

Figure 5a shows that net energy productions were possible in the system during most of the operating period, when treating a wastewater with a COD content above 1 $g \cdot L^{-1}$. Although the main wastewater source was UWW, there was also an industrial contribution increasing both organic and sulfate loads to the AnMBR. Therefore, it is also worth to point out that there was a strong competition between methanogens and SRB for the available substrate due to the high sulfate concentration in the influent to the system. Enhanced energy recoveries would have been achieved if treating lower

sulfate loads.

Regarding dissolved methane recovery, the degassing membranes also resulted in net energy productions, which enabled to slightly enhance the energy balance of the plant. However, the recovered dissolved methane contribution was not significant to the overall energy production (data not shown). Therefore, the main benefit of the installed degassing membranes is a reduction of the carbon footprint of the AnMBR.

Figure 5b shows the GHG emissions calculated during the operating phase. As this figure shows, dissolved methane in the effluent is the main contributor to GHG emissions as long as dissolved methane is not captured, stating the relevance of methane recovery from the effluent. When dissolved methane is captured by means of degassing membranes, GHG emissions are noticeably reduced. Indeed, emissions around zero were determined during the experimental period, as mild and warmer climate conditions reduced methane solubility, allowing to recover most of produced methane in the biogas stream. Indeed, above 90% of total methane was recovered in the biogas in this study. Further details on the energy balance and the carbon footprint of this AnMBR plant can be found in Jiménez-Benítez et al. (2020).

The presence of nutrients (mainly N and P) in the effluent of AnMBR systems, jointly with the high quality of the water, makes possible the use of the produced permeate for fertigation purposes (simultaneous reuse of water and nutrients), an attractive approach for resource recovery (Jimenez et al., 2020 submitted). Fertigation allows conserving freshwater sources and decreasing energy consumption for inorganic ammonia-based fertilizer production (19.3 kWh per kg N by the Haber-Bosh process according to

McCarty et al. (2011)) and P extraction (2.1 kWh per kg P according to Gellings and Parmenter (2004)). It should also be taken into account that P was included in the EU's Critical Raw Materials list in 2017 (European Commission, 2017). If accounting for the energy savings derived from using the AnMBR effluent for fertirrigation instead of inorganic fertilizers, the net energy demand of the AnMBR would be reduced in around 0.95 kWh per m^3 of water reused. This is obtained from the energy consumption for inorganic ammonia-based fertilizer production (19.3 kWh per kg N) and P extraction (2.1 kWh per kg P according), and the concentrations of N and P in the AnMBR effluent (48 ±6 mg $N \cdot L^{-1}$ and 9 ± 2 mg $P \cdot L^{-1}$). Regarding carbon footprint, the GHG emissions of the AnMBR would be reduced in 0.37 kg CO_2 per m^3 of water reused when using the AnMBR effluent for fertirrigation, based on the Spanish electricity emission factor of 0.392 kgCO_2 per kWh and the energy saving of 0.95 kWh per m^3 of water reused for fertirrigation. When considering an European average electricity specific emission factor of 0.2958 kg CO_2 per kWh (EEA, 2018), the GHG emissions of the AnMBR would be reduced in 0.28 kg CO_2 per m^3 of water reused instead of 0.37 kg CO_2 per m^3 of water reused. Furthermore, due to the high quality of AnMBR effluent (low organic content, free of suspended solids), tertiary treatment and associated energy demand and GHG emissions could be avoided. Therefore, AnMBR technology is a suitable approach for UWW when existing fertigation water demand.

4. Conclusions

An industrial AnMBR prototype was operated for 350 days. Following an around 100-day start-up period, the system remained virtually unchanged, stating its robustness against disturbances. Additionally, COD-discharge limits were mostly met, resulting in

an average COD removal of 92%. Most of the COD was removed biologically reducing the sludge production by 36-58% compared to CAS. The filtration process performance was satisfactory, with low power requirements (0.15 kWh per m^3 of treated water) whilst producing a nutrient-rich, pathogens-free permeate. Net energy production was possible during most of the operating period, with negligible GHG emissions as long as dissolved methane was captured.

E-supplementary data of this work can be found in online version of the paper

Acknowledgement

The authors are grateful to the European Commission for the co-financing of the LIFE MEMORY project (LIFE13 ENV/ES/ 001353) and the staff of Aguas de Alcázar for their collaboration.

References

1. APHA, 2005. Standard Methods for the Examination of Water and Wastewater. American Public Health Association, Washington, DC.

2. Aslam, M., McCarty, P.L., Shin, C., Bae, J., Kim, J., 2017. Low energy single-staged anaerobic fluidized bed ceramic membrane bioreactor (AFCMBR) for wastewater treatment. Bioresour. Technol. 240, 33–41. https://doi.org/10.1016/j.biortech.2017.03.017

3. Batstone, D.J., Virdis, B., 2014. The role of anaerobic digestion in the emerging energy economy. Curr. Opin. Biotechnol. 27, 142–149. https://doi.org/10.1016/j.copbio.2014.01.013

4. Becker, A.M., Yu, K., Stadler, L.B., Smith, A.L., 2017. Co-management of domestic wastewater and food waste: A life cycle comparison of alternative food waste diversion strategies. Bioresour. Technol. 223, 131–140. https://doi.org/10.1016/j.biortech.2016.10.031

5. Dereli, R.K., Ersahin, M.E., Ozgun, H., Ozturk, I., Jeison, D., van der Zee, F., van Lier, J.B., 2012. Potentials of anaerobic membrane bioreactors to overcome treatment limitations induced by industrial wastewaters. Bioresour. Technol. 122, 160–170. https://doi.org/10.1016/j.biortech.2012.05.139

6. EEA, 2018. Water use and environmental pressures [WWW Document].

7. Eggleston H.S., Buendia L., Miwa K., N.T. and T.K., 2006. IPCC Guidelines for National Greenhouse Gas Inventories.

8. European Commission, 2017. Communication from the Commission to the European Parliament, the Council, the European Economic and Social Committee and the Committee of the Regions: on the 2017 list of Critical Raw Materials for the EU, Official Journal of the European Union. Brussels (Belgium).

9. Fedorovich, V., Lens, P., Kalyuzhnyi, S., 2003. Extension of Anaerobic Digestion Model No. 1 with Processes of Sulfate Reduction. Appl. Biochem. Biotechnol. 109, 33–46. https://doi.org/10.1385/ABAB:109:1-3:33

10. Foladori, P., Andreottola, G., Ziglio, G., 2010. Sludge Reduction Technologies in Wastewater Treatment Plants. https://doi.org/10.2166/9781780401706

11. Galib, M., Elbeshbishy, E., Reid, R., Hussain, A., Lee, H.S., 2016. Energy-positive food wastewater treatment using an anaerobic membrane bioreactor (AnMBR). J. Environ. Manage. 182, 477–485. https://doi.org/10.1016/j.jenvman.2016.07.098

12. Gellings, C.W., Parmenter, K.E., 2004. Energy efficiency in fertilizer production and use. In Knowledge for Sustainable Development—An Insight into the Encyclopedia of Life Support Systems. Eolss Publishers, Oxford.

13. Giménez, J.B., Martí, N., Ferrer, J., Seco, A., 2012. Methane recovery efficiency in a submerged anaerobic membrane bioreactor (SAnMBR) treating sulphate-rich urban wastewater: Evaluation of methane losses with the effluent. Bioresour. Technol. 118, 67–72. https://doi.org/10.1016/j.biortech.2012.05.019

14. Giménez, J.B., Robles, A., Carretero, L., Durán, F., Ruano, M.V., Gatti, M.N., Ribes, J., Ferrer, J., Seco, A., 2011. Experimental study of the anaerobic urban wastewater treatment in a submerged hollow-fibre membrane bioreactor at pilot scale. Bioresour. Technol. 102, 8799–8806. https://doi.org/10.1016/J.BIORTECH.2011.07.014

15. Gouveia, J., Plaza, F., Garralon, G., Fdz-Polanco, F., Peña, M., 2015. Long-term operation of a pilot scale anaerobic membrane bioreactor (AnMBR) for the treatment of municipal wastewater under psychrophilic conditions. Bioresour. Technol. 185, 225–233. https://doi.org/10.1016/J.BIORTECH.2015.03.002

16. Günther, S., Grunert, M., Müller, S., 2018. Overview of recent advances in phosphorus recovery for fertilizer production. Eng. Life Sci.

https://doi.org/10.1002/elsc.201700171

17. Harb, M., Hong, P.Y., 2017. Anaerobic membrane bioreactor effluent reuse: A review of microbial safety concerns. Fermentation 3. https://doi.org/10.3390/fermentation3030039

18. Huijbregts, M., Steinmann, Z.J.N., Elshout, P.M.F.M., Stam, G., Verones, F., Vieira, M.D.M., Zijp, M., van Zelm, R., 2016. ReCiPe 2016. Natl. Inst. Public Heal. Environ. 194. https://doi.org/10.1007/s11367-016-1246-y

19. Ince, O., Gurol, Z.C., Ozbayram, E.G., Iglesias, M.M., Ince, B., Massalha, N., Robles, Á., Sabbah, I., Seco, A., 2017. Anaerobic treatment of municipal wastewater. Innov. Wastewater Treat. & Resour. Recover. Technol. Impacts Energy, Econ. Environ. https://doi.org/10.2166/9781780407876_0040

20. Jiménez-Benítez, A., Ferrer, J., Rogalla, F., Vázquez, J.R., Seco, A., Robles, Á., 2020. 12 - Energy and environmental impact of an anaerobic membrane bioreactor (AnMBR) demonstration plant treating urban wastewater, in: Mannina, G., Pandey, A., Larroche, C., Ng, H.Y., Ngo, H.H.B.T.-C.D. in B. and B. (Eds.), . Elsevier, pp. 289–310. https://doi.org/https://doi.org/10.1016/B978-0-12-819854-4.00012-5

21. Kamali, M., Khodaparast, Z., 2015. Review on recent developments on pulp and paper mill wastewater treatment. Ecotoxicol. Environ. Saf. 114, 326–342. https://doi.org/10.1016/j.ecoenv.2014.05.005

22. Kim, J., Kim, K., Ye, H., Lee, E., Shin, C., McCarty, P.L., Bae, J., 2011. Anaerobic Fluidized Bed Membrane Bioreactor for Wastewater Treatment.

Environ. Sci. Technol. 45, 576–581. https://doi.org/10.1021/es1027103

23. Krzeminski, P., Katsou, E., Dosoretz, C.G., Esteban-García, A.L., Leverette, L., Malamis, S., Nenov, V., Robles, Á., Seco, A., Syron, E., 2017. Membranes in wastewater treatment. Innov. Wastewater Treat. & Resour. Recover. Technol. Impacts Energy, Econ. Environ. https://doi.org/10.2166/9781780407876_0129

24. Lee, M., Keller, A.A., Chiang, P.C., Den, W., Wang, H., Hou, C.H., Wu, J., Wang, X., Yan, J., 2017. Water-energy nexus for urban water systems: A comparative review on energy intensity and environmental impacts in relation to global water risks. Appl. Energy 205, 589–601. https://doi.org/10.1016/j.apenergy.2017.08.002

25. Lens, P.N.L., Visser, a., Janssen, a. J.H., Pol, L.W.H., Lettinga, G., 1998. Biotechnological Treatment of Sulfate-Rich Wastewaters. Crit. Rev. Environ. Sci. Technol. 28, 41–88. https://doi.org/10.1080/10643389891254160

26. Lew, B., Lustig, I., Beliavski, M., Tarre, S., Green, M., 2011. An integrated UASB-sludge digester system for raw domestic wastewater treatment in temperate climates. Bioresour. Technol. 102, 4921–4924. https://doi.org/10.1016/j.biortech.2011.01.030

27. Li, X., Wang, X., 2006. Modelling of membrane fouling in a submerged membrane bioreactor. J. Memb. Sci. 278, 151–161. https://doi.org/10.1016/J.MEMSCI.2005.10.051

28. Maree, J.P., Strydom, W.F., 1985. Biological sulphate removal in an upflow

packed bed reactor. Water Res. 19, 1101–1106. https://doi.org/https://doi.org/10.1016/0043-1354(85)90346-X

29. Martin Garcia, I., Mokosch, M., Soares, A., Pidou, M., Jefferson, B., 2013. Impact on reactor configuration on the performance of anaerobic MBRs: Treatment of settled sewage in temperate climates. Water Res. 47, 4853–4860. https://doi.org/10.1016/J.WATRES.2013.05.008

30. Martin, I., Pidou, M., Soares, A., Judd, S., Jefferson, B., 2011. Modelling the energy demands of aerobic and anaerobic membrane bioreactors for wastewater treatment. Environ. Technol. 32, 921–932. https://doi.org/10.1080/09593330.2011.565806

31. Martinez-Sosa, D., Helmreich, B., Netter, T., Paris, S., Bischof, F., Horn, H., 2011. Anaerobic submerged membrane bioreactor (AnSMBR) for municipal wastewater treatment under mesophilic and psychrophilic temperature conditions. Bioresour. Technol. 102, 10377–10385. https://doi.org/10.1016/J.BIORTECH.2011.09.012

32. McCarty, Perry L, Bae, J., Kim, J., 2011. Domestic Wastewater Treatment as a Net Energy Producer–Can This be Achieved? Environ. Sci. Technol. 45, 7100–7106. https://doi.org/10.1021/es2014264

33. McCarty, Perry L., Bae, J., Kim, J., 2011. Domestic wastewater treatment as a net energy producer-can this be achieved? Environ. Sci. Technol. 45, 7100–7106. https://doi.org/10.1021/es2014264

34. Mitchell, J., Weir, M.H., Rose, J., n.d. Quantitative microbial risk assessment

[WWW Document]. Quant. Microb. risk Assess. URL http://qmrawiki.org/ (accessed 6.12.20).

35. Moosbrugger, R.E., Wentzel, M.C., Ekama, G.A., Marais, G., 1992. Simple titration procedures to determine H2CO3* alkalinity and short-chain fatty acids in aqueous solutions. Pretoria.

36. Ozgun, H., Dereli, R.K., Ersahin, M.E., Kinaci, C., Spanjers, H., Van Lier, J.B., 2013. A review of anaerobic membrane bioreactors for municipal wastewater treatment: Integration options, limitations and expectations. Sep. Purif. Technol. 118, 89–104. https://doi.org/10.1016/j.seppur.2013.06.036

37. Robles, Á., Aguado, D., Barat, R., Borrás, L., Bouzas, A., Bautista Giménez, J., Martí, N., Ribes, J., Victoria Ruano, M., Serralta, J., Ferrer, J., Seco, A., 2019. New frontiers from removal to recycling of nitrogen and phosphorus from wastewater in the circula economy. Bioresour. Technol. 122673. https://doi.org/10.1016/J.BIORTECH.2019.122673

38. Robles, A., Durán, F., Ruano, M.V., Ribes, J., Rosado, A., Seco, A., Ferrer, J., 2015. Instrumentation, control, and automation for submerged anaerobic membrane bioreactors. Environ. Technol. (United Kingdom) 36. https://doi.org/10.1080/09593330.2015.1012180

39. Robles, Á., Ruano, M.V., Charfi, A., Lesage, G., Heran, M., Harmand, J., Seco, A., Steyer, J.-P., Batstone, D.J., Kim, J., Ferrer, J., 2018. A review on anaerobic membrane bioreactors (AnMBRs) focused on modelling and control aspects. Bioresour. Technol. 270, 612–626.

https://doi.org/10.1016/J.BIORTECH.2018.09.049

40. Sanchis-Perucho, P., Robles, Á., Durán, F., Ferrer, J., Seco, A., 2020. PDMS membranes for feasible recovery of dissolved methane from AnMBR effluents. J. Memb. Sci. 604, 118070. https://doi.org/https://doi.org/10.1016/j.memsci.2020.118070

41. Seco, A., Mateo, O., Zamorano-López, N., Sanchis-Perucho, P., Serralta, J., Martí, N., Borrás, L., Ferrer, J., 2018a. Exploring the limits of anaerobic biodegradability of urban wastewater by AnMBR technology. Environ. Sci. Water Res. Technol. 4, 1877–1887. https://doi.org/10.1039/c8ew00313k

42. Seco, A., Aparicio, S., González-Camejo, J., Jiménez-Benítez, A., Mateo, O., Mora, J.F., Noriega-Hevia, G., Sanchis-Perucho, P., Serna-García, R., Zamorano-López, N., Giménez, J.B., Ruiz-Martinez, A., Aguado, D., Barat, R., Borrás, L., Bouzas, A., Martí, N., Pachés, M., Ribes, J., Robles, A., Ruano, M.V., Serralta, J. and Ferrer, J., 2018b. Resource recovery from sulphate-rich sewage through an innovative anaerobic-based water resource recovery facility (WRRF). Water Sci. Technol. 78 (9), 1925-1936. https://doi.org/10.2166/wst.2018.492

43. Shin, C., Bae, J., 2018. Current status of the pilot-scale anaerobic membrane bioreactor treatments of domestic wastewaters: A critical review. Bioresour. Technol. 247, 1038–1046. https://doi.org/10.1016/j.biortech.2017.09.002

44. Shin, C., McCarty, P.L., Kim, J., Bae, J., 2014. Pilot-scale temperate-climate treatment of domestic wastewater with a staged anaerobic fluidized membrane

bioreactor (SAF-MBR). Bioresour. Technol. 159, 95–103. https://doi.org/10.1016/J.BIORTECH.2014.02.060

45. Smith, A.L., Stadler, L.B., Love, N.G., Skerlos, S.J., Raskin, L., 2012. Perspectives on anaerobic membrane bioreactor treatment of domestic wastewater: A critical review. Bioresour. Technol. 122, 149–159. https://doi.org/10.1016/j.biortech.2012.04.055

46. Song, X., Luo, W., Hai, F.I., Price, W.E., Guo, W., Ngo, H.H., Nghiem, L.D., 2018. Resource recovery from wastewater by anaerobic membrane bioreactors: Opportunities and challenges. Bioresour. Technol. https://doi.org/10.1016/j.biortech.2018.09.001

47. Stazi, V., Tomei, M.C., 2018. Enhancing anaerobic treatment of domestic wastewater: State of the art, innovative technologies and future perspectives. Sci. Total Environ. 635, 78–91. https://doi.org/10.1016/j.scitotenv.2018.04.071

48. van Lier, J.B., Seco, A., Jefferson, B., Ersahin, M.E., Robles, A., 2019. Upgrading anaerobic sewage treatment applying membranes: AnMBR and UF post filtration. Anaerob. React. Sew. Treat. Des. Constr. Oper. https://doi.org/10.2166/9781780409238_0339

49. Wang, K.M., Jefferson, B., Soares, A., McAdam, E.J., 2018. Sustaining membrane permeability during unsteady-state operation of anaerobic membrane bioreactors for municipal wastewater treatment following peak-flow. J. Memb. Sci. 564, 289–297. https://doi.org/10.1016/J.MEMSCI.2018.07.032

Figure and table captions

Figure 1. (a) Flow diagram of the AnMBR Plant, and (b) AnMBR plant overview. Note: "n" represents the membrane treatment lane.

Figure 2. Evolution of: **(a)** TSS concentration in the reactor, VFA concentration in the effluent, methane content in the biogas, and temperature in the reactor; and **(b)** influent and effluent COD concentration, and COD removal efficiency.

Figure 3. Evolution of: (a) sludge production and methane yield; and (b) total COD biodegraded and COD removal by sulfate reducing organisms.

Figure 4. Evolution of: **(a)** TSS, SGD_P and J_{20}; **(b)** TMP and K_{20}; and **(c)** FR_C. MT-A and MT-B refer to membrane tanks A and B, respectively.

Figure 5. Evolution of **(a)** the net energy demand and **(b)** the GHG emissions from the operating phase of the demonstration plant.

Table 1. Operating conditions set during the experimental period.

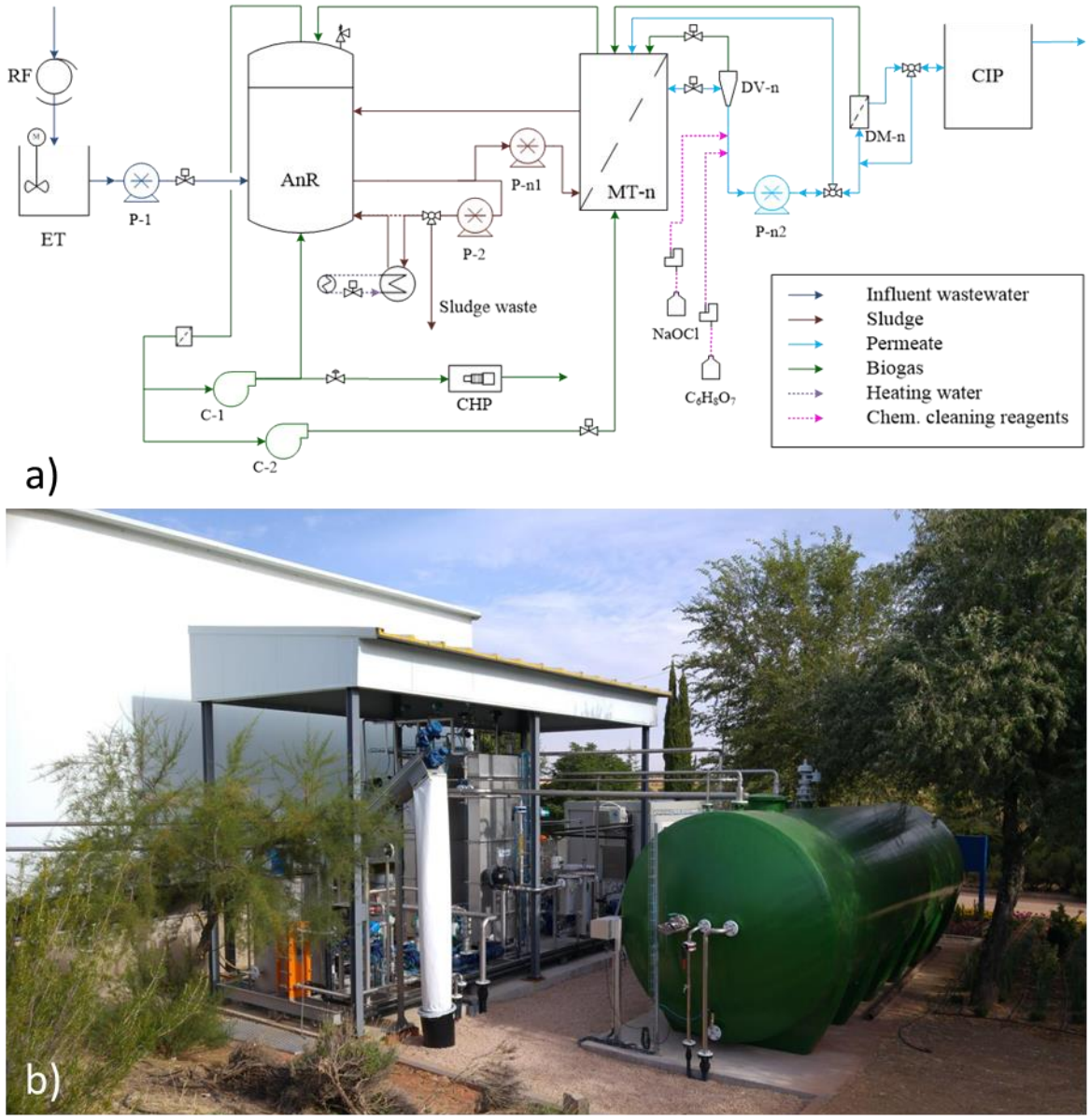
RF
ET
P-1
AnR
P-n1
P-2
Sludge waste
MT-n
DV-n
DM-n
CIP
P-n2
NaOCl
$C_6H_8O_7$
C-1
C-2
CHP
Influent wastewater
Sludge
Permeate
Biogas
Heating water
Chem. cleaning reagents
a)
b)

Figure 2

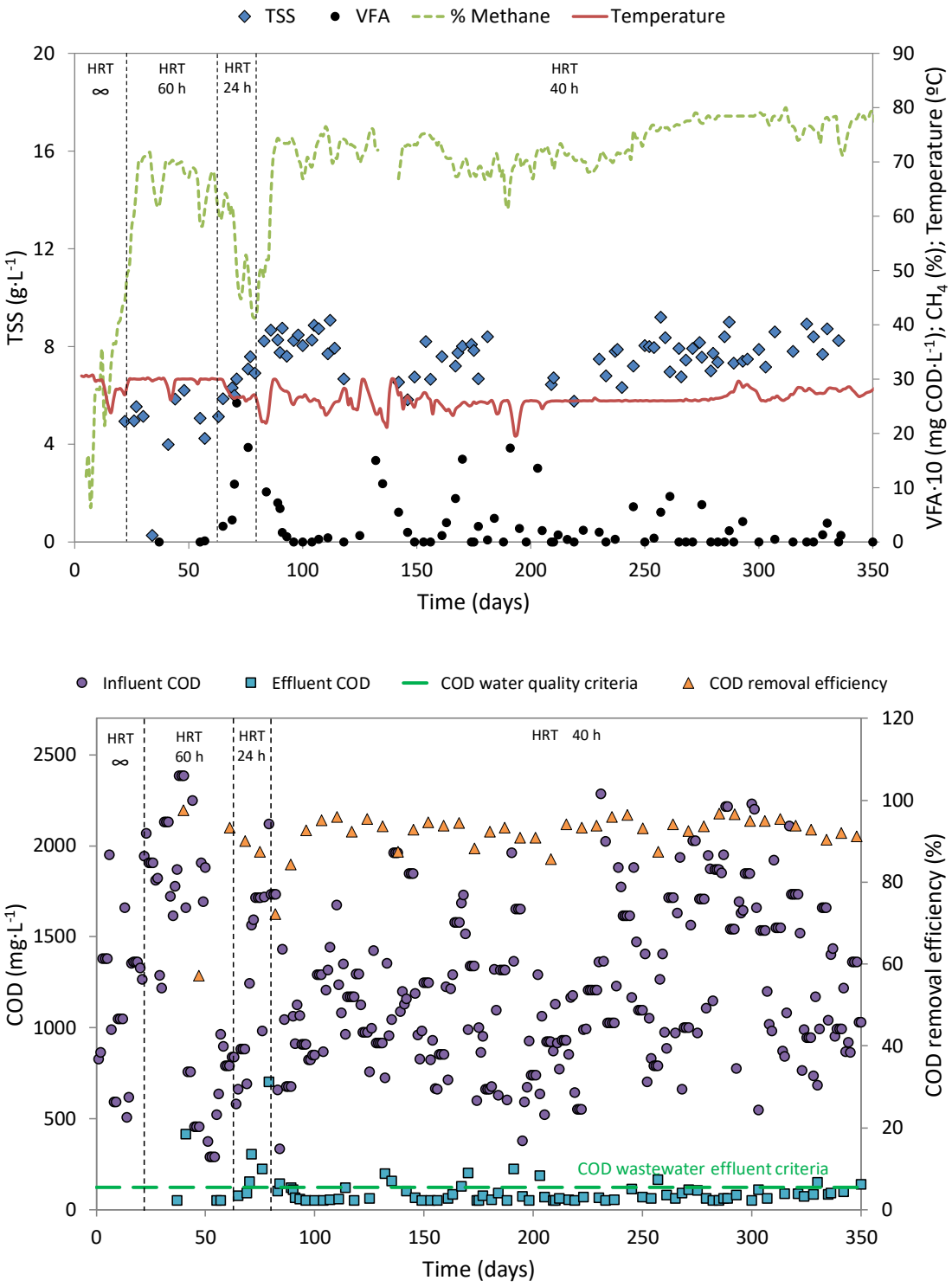
TSS
VFA
% Methane
Temperature
HRT ∞
HRT 60 h
HRT 24 h
HRT 40 h
TSS (g·L-1)
VFA·10 (mg COD·L-1); CH4 (%); Temperature (ºC)
Time (days)
Influent COD
Effluent COD
COD water quality criteria
COD removal efficiency
COD (mg·L-1)
COD removal efficiency (%)
COD wastewater effluent criteria

Figure 2

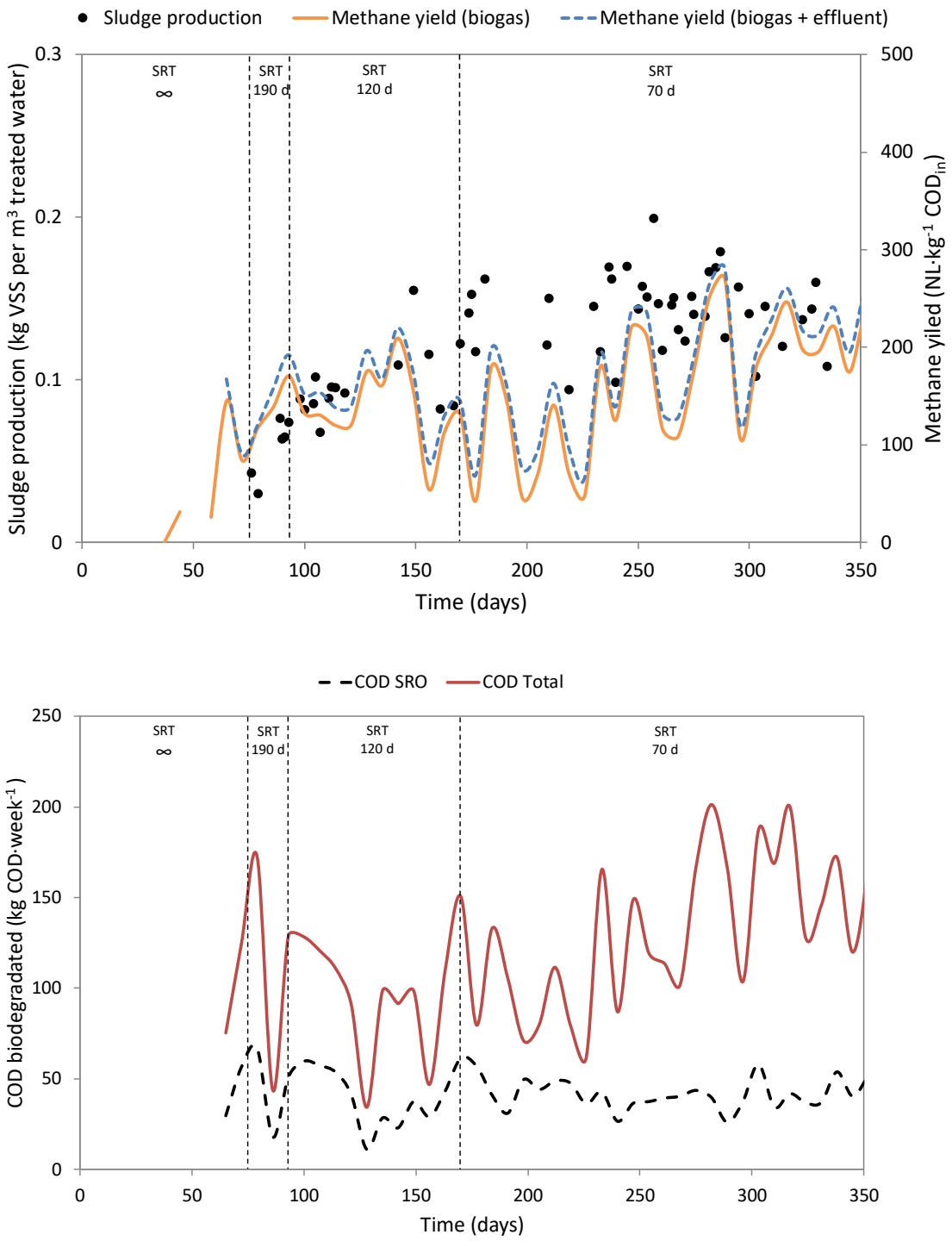
Sludge production
Methane yield (biogas)
Methane yield (biogas + effluent)
SRT ∞
SRT 190 d
SRT 120 d
SRT 70 d
Sludge production (kg VSS per m3 treated water)
Methane yiled (NL·kg-1 CODin)
Time (days)
COD SRO
COD Total
COD biodegradated (kg COD·week-1)

Figure 3

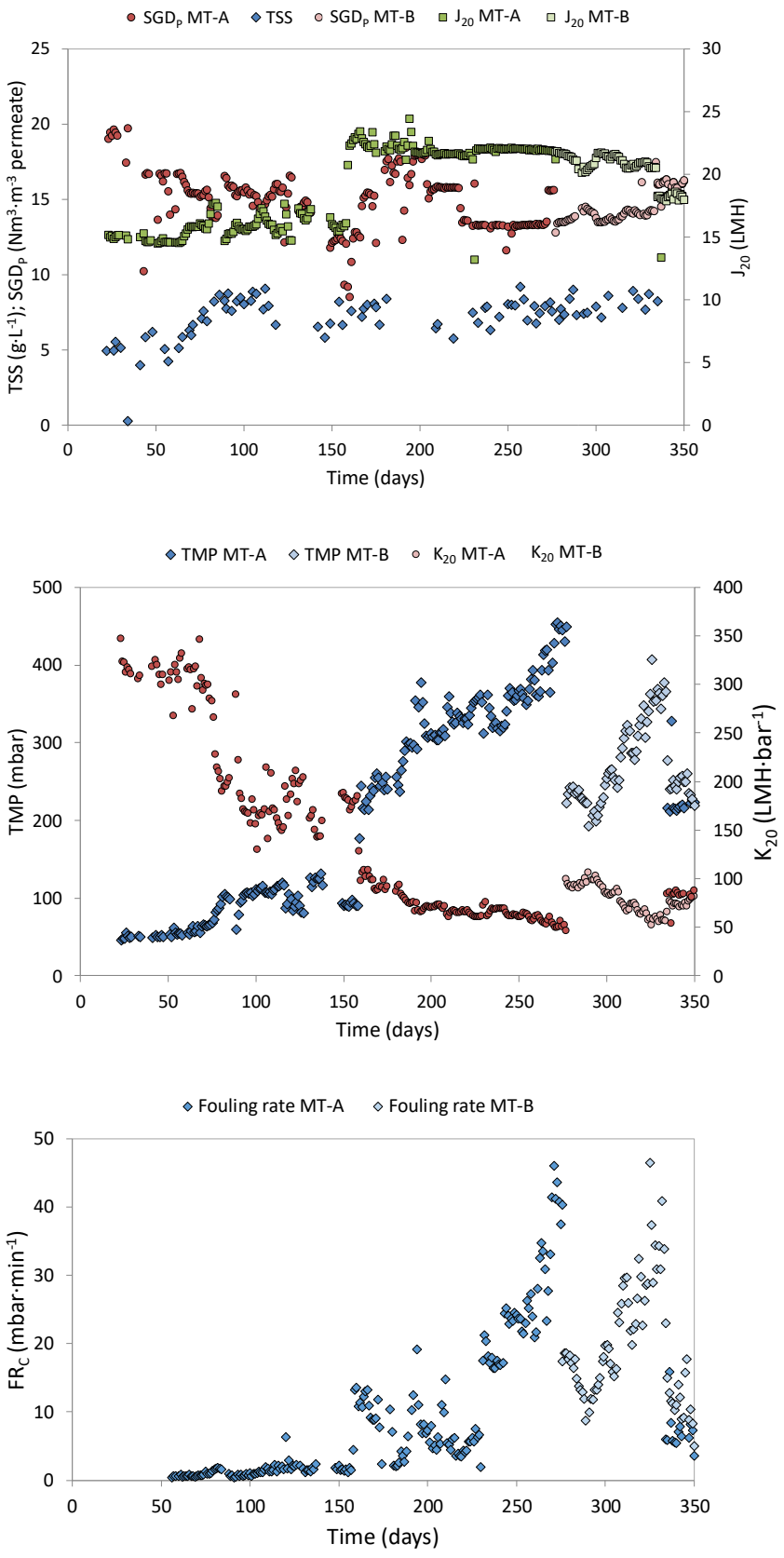
SGDp MT-A
TSS
SGDp MT-B
J20 MT-A
J20 MT-B
TSS (g·L-1); SGDp (Nm3·m-3 permeate)
J20 (LMH)
Time (days)
TMP MT-A
TMP MT-B
K20 MT-A
K20 MT-B
TMP (mbar)
K20 (LMH·bar-1)
Time (days)
Fouling rate MT-A
Fouling rate MT-B
FRC (mbar·min-1)
Time (days)

Figure 4

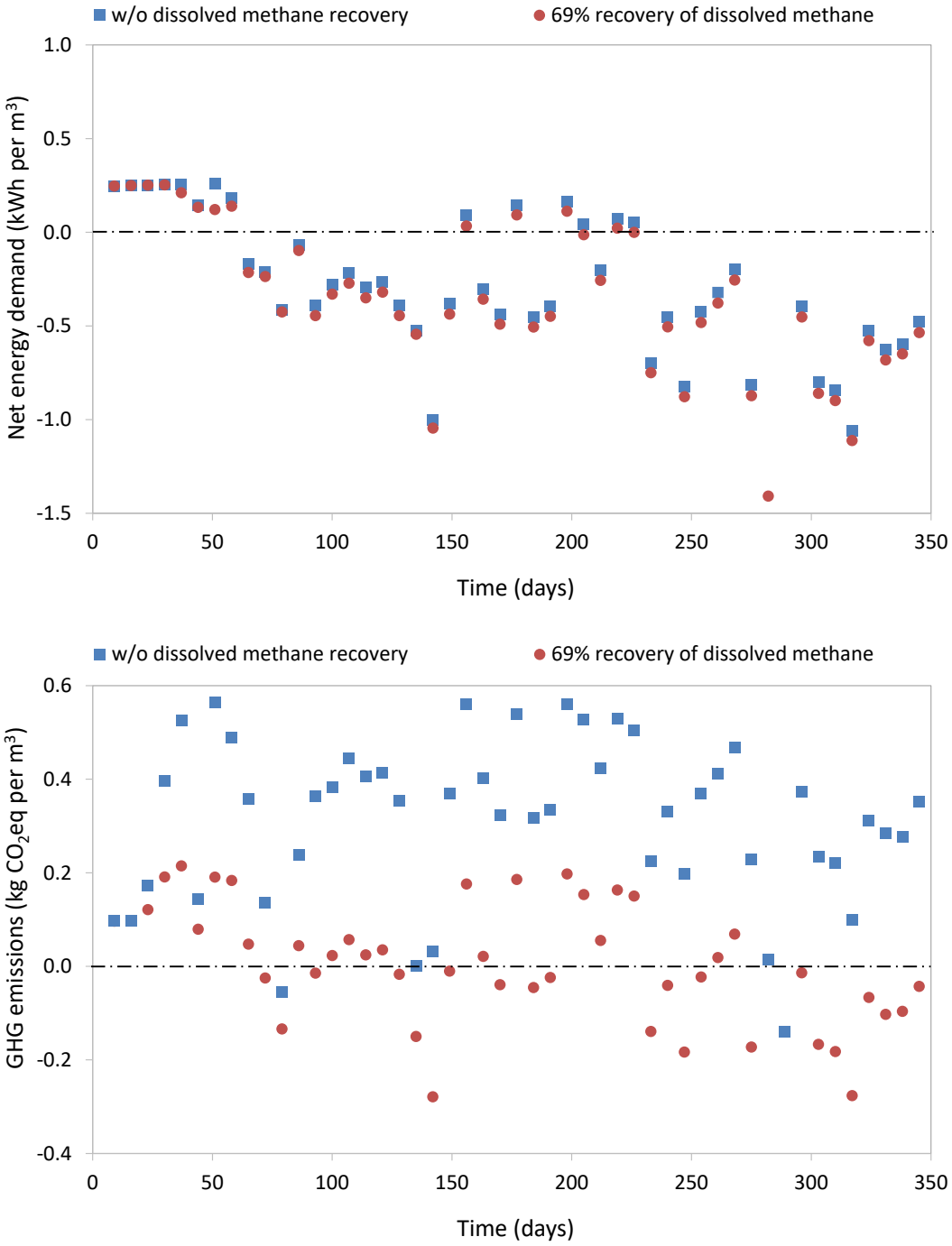
w/o dissolved methane recovery
69% recovery of dissolved methane
Net energy demand (kWh per m³)
1.0
0.5
0.0
-0.5
-1.0
-1.5
0
50
100
150
200
250
300
350
Time (days)
w/o dissolved methane recovery
69% recovery of dissolved methane
GHG emissions (kg CO2eq per m³)
0.6
0.4
0.2
0.0
-0.2
-0.4
0
50
100
150
200
250
300
350
Time (days)

Figure 5

Table 1

Time (days)	HRT (h)	SRT (d)	J (LMH)	SGD_P ($Nm^3_{BIOGAS} \cdot m^{-3}_{PERMEATE}$)
1 : 25	∞	∞	15 - 17	12 - 17
25 : 65	60			
65 : 80	24			
80 : 95	40	190		
95 : 160		120		
160 : 170			20.5 - 23.5	17.5 - 13
170 : 335		70		
335 : 350			18	16

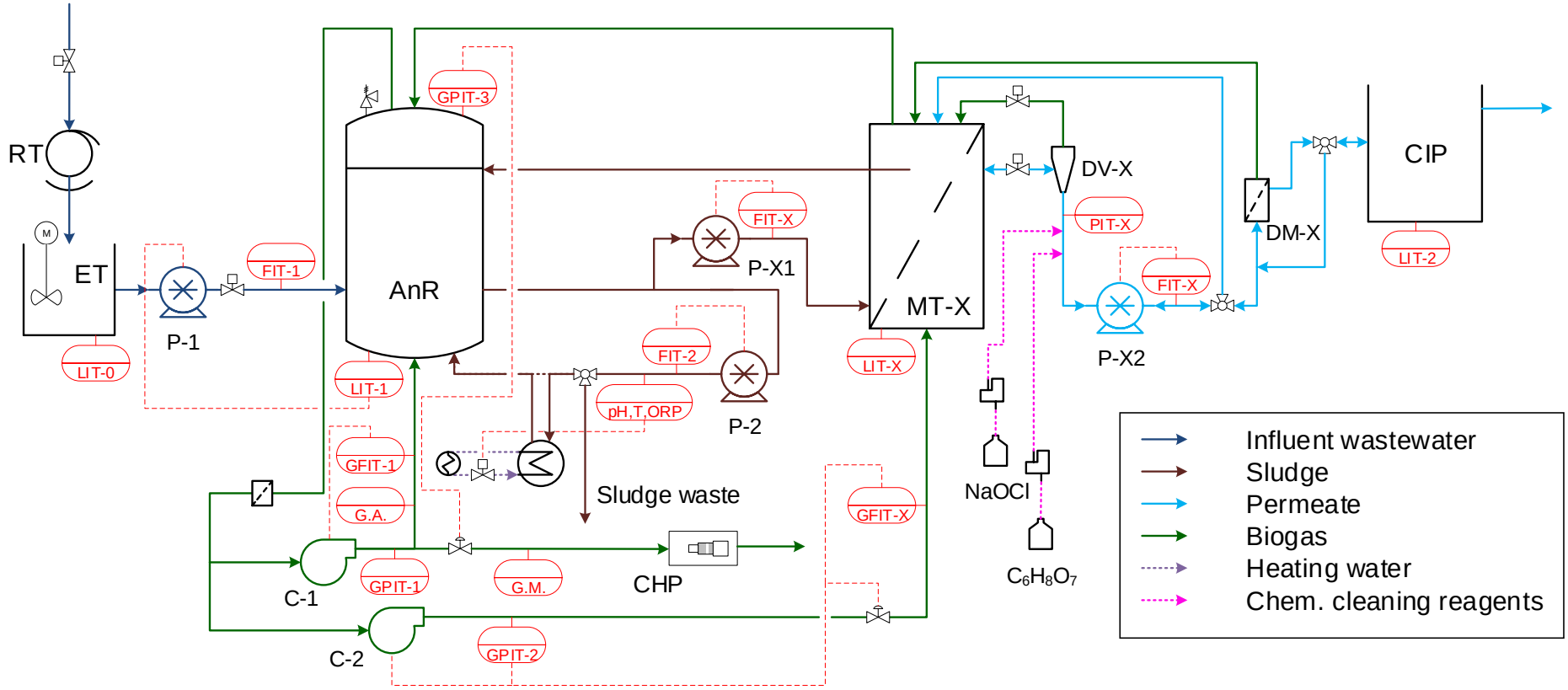
RT
ET
M
LIT-0
P-1
FIT-1
AnR
GPIT-3
LIT-1
FIT-2
P-2
pH,T,ORP
P-X1
FIT-X
MT-X
LIT-X
DV-X
PIT-X
FIT-X
P-X2
DM-X
CIP
LIT-2
GFIT-1
G.A.
GPIT-1
G.M.
C-1
C-2
GPIT-2
Sludge waste
CHP
GFIT-X
NaOCl
$C_6H_8O_7$
Influent wastewater
Sludge
Permeate
Biogas
Heating water
Chem. cleaning reagents

Figure S1. Process and Instrumentation Diagram.

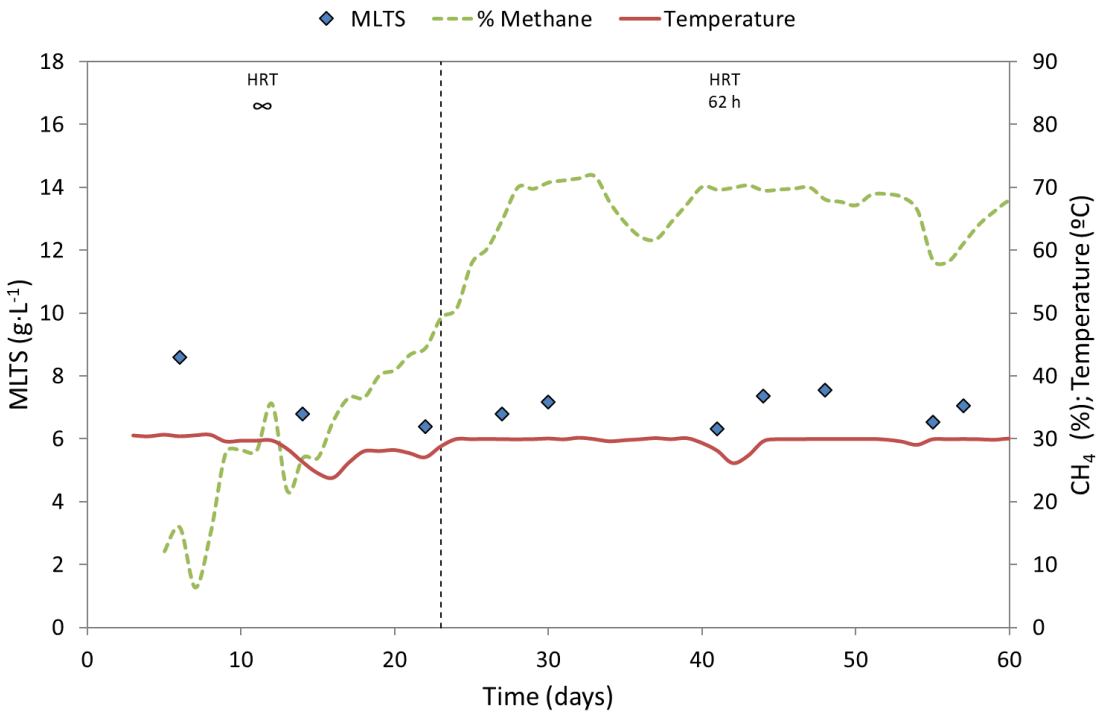

Figure S2. Evolution during the start-up period of the MLTS in the anaerobic reactor, the methane content in the biogas and the reactor temperature.

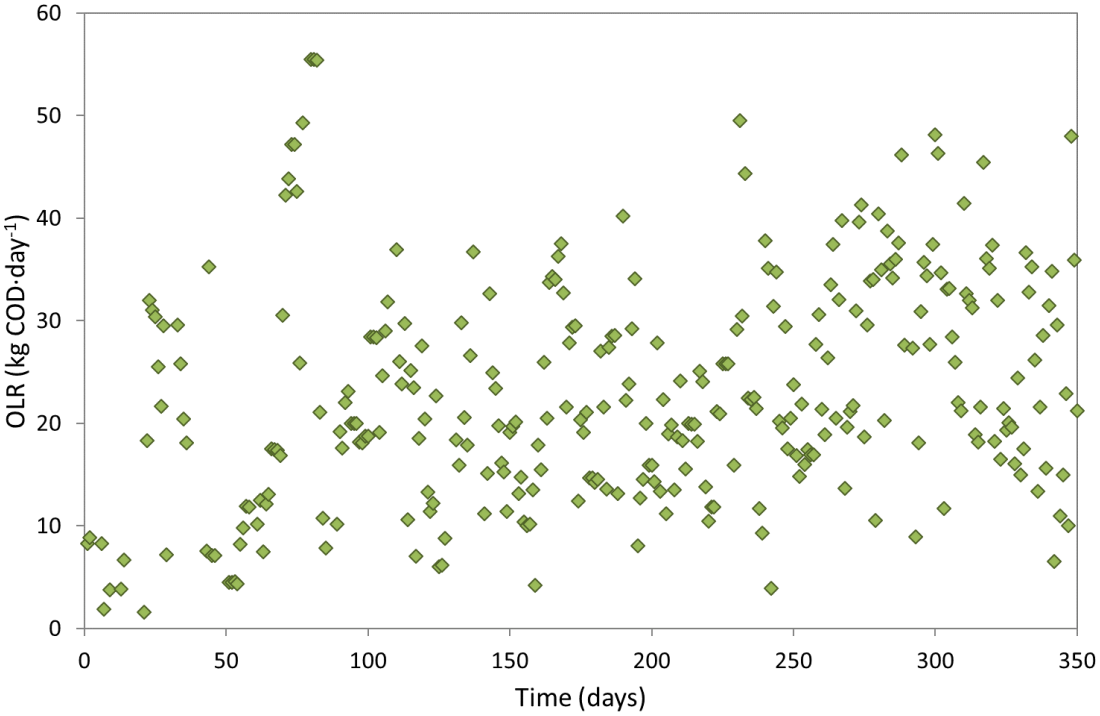

Figure S3. Evolution of the organic loading rate entering the AnMBR.

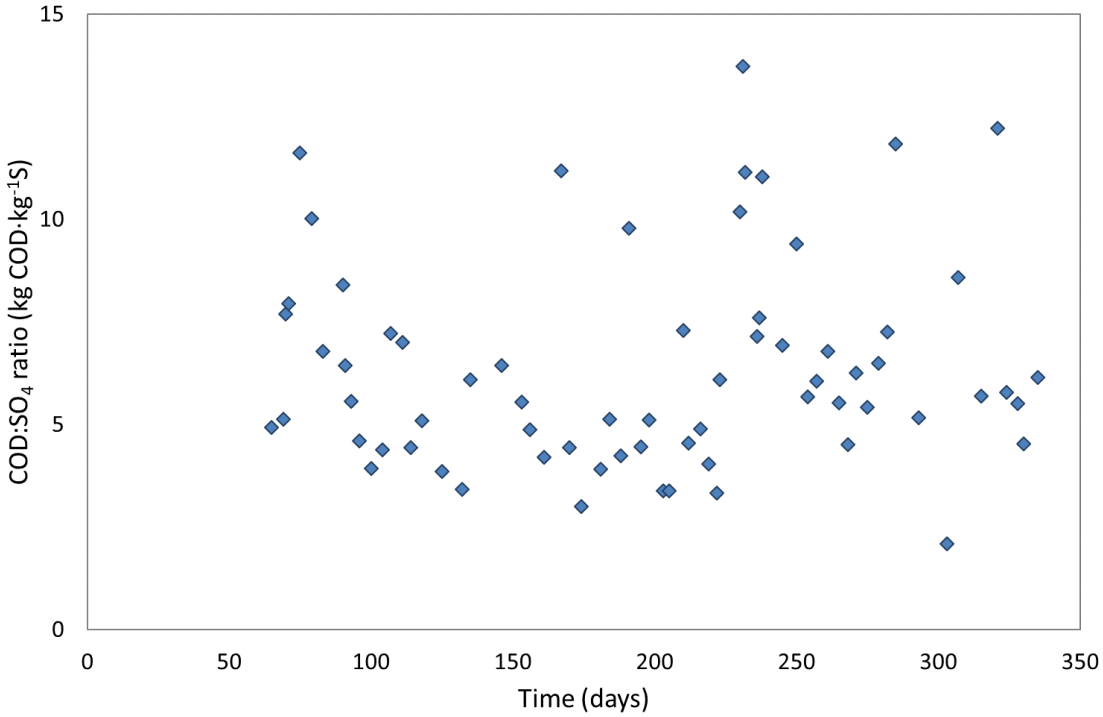

Figure S4. Evolution of the COD:SO_4-S ratio entering the AnMBR expressed as kg COD per kg of sulfur.

Table S1. Average influent wastewater characteristics.

Parameter	**Unit**	**Mean ± SD**
TSS	mg $TSS \cdot L^{-1}$	536 ± 248
Total COD	mg $COD \cdot L^{-1}$	1235 ± 462
BOD_5	mg $COD \cdot L^{-1}$	694 ± 281
Total Nitrogen	mg $N \cdot L^{-1}$	56.5 ± 17.0
Total Phosphorus	mg $P \cdot L^{-1}$	10.1 ± 3.2
Sulfate	mg $SO_4\text{-}S \cdot L^{-1}$	164.4 ± 31.3
Alkalinity	mg $CaCO_3 \cdot L^{-1}$	613 ± 124
VFA	mg $COD \cdot L^{-1}$	111 ± 85